Textures and Microstructures, 1991, Vol. 13, pp. 133–154
Reprints available directly from the publisher.
Photocopying permitted by license only

MICROSTRUCTURE AND TEXTURE EVOLUTION DURING THE ANNEALING OF COLD-WORKED Zr-1 wt%Nb

DEREK O. NORTHWOOD and JOHN W. ROBINSON

Engineering Materials Group, University of Windsor, Windsor, Ontario, Canada N9B 3P4

and

ZHENG JIE

General Research Institute for Non-Ferrous Metals, Beijing, People's Republic of China

The texture changes in tube reduced (60%) and stress relieved Zr-1 wt%Nb nuclear fuel sheathing on annealing at temperatures from 300–1100°C for 10^4 seconds have been measured using an X-ray inverse pole figure technique. These changes in texture are then related to changes in both mechanical anisotropy as determined using Knoop microhardness measurements and microstructure as seen using optical metallography. Changes in texture and anisotropy arise both from recrystallization and phase changes, with major texture changes only occurring at temperatures where there is a phase transformation to β_{Zr}.

KEY WORDS Zr-1 wt%Nb, annealing, texture, microstructure, mechanical anisotropy.

INTRODUCTION

Ever since the Second Geneva Conference on the Peaceful Uses of Atomic Energy in 1958 there has been increasing interest in the use of zirconium-niobium alloys as structural and fuel sheathing materials in water-cooled nuclear reactors. The USSR was the first to develop these alloys and they have promoted the use of a Zr-1 wt%Nb alloy for fuel sheathing applications (Amaev *et al.*, 1964, 1966, 1968). An alloy containing 2.5 wt%Nb which was also originally developed in the USSR, has been extensively used in CANDU-PHW reactors for the fabrication of pressure tubes (Northwood, 1985).

Although the Zr-1 wt%Nb alloy has not found any extensive usage outside the USSR and associated countries, there is interest in its use as a fuel sheathing in place of the more commonly used Zircaloys (Zr-Sn alloys) because of its better corrosion resistance at high temperatures, particularly in a boiling water environment, less radiation enhanced corrosion and excellent post-irradiation ductility (Northwood, 1974).

The Zr-1 wt%Nb fuel sheathing is commonly used in the cold-worked (tube reduced) condition. In this metallurgical condition tubing exhibits mechanical anisotropy both from the cold work and from crystallographic factors (h.c.p.

structure). During in-reactor service the anisotropy can change because of removal of cold work, activation of new slip systems or phase (microstructural) changes. The temperature range of interest is from 300°C, reactor operating temperatures for CANDU-PHWs, to about 1100°C which is the temperature reached during occurrences such as a postulated loss-of-coolant accident (LOCA). The aim of the present study is to follow the changes in anisotropy produced by annealing at temperatures from 300°C to 1100°C using Knoop microhardness (mechanical anisotropy), X-ray texture measurements (crystallographic anisotropy) and optical metallography (microstructural changes). Some initial results together with the complementary thermoelectric power measurements have already been published (Jie, Robinson & Northwood, 1989).

EXPERIMENTAL DETAILS

Materials

The material used in this study was as-fabricated Zr-1 wt%Nb fuel sheathing. The tubing was in the 60% tube-reduced and stress-relieved condition. The tubing size was 13.4 mm outside diameter and 0.4 mm wall thickness. The complete chemical analysis is given in Table 1. Short sections of tubing were cut and these were used for optical metallographic, microhardness and texture specimens.

Heat Treatment

The samples were sealed in vacuum-evacuated quartz tubes for heat treatment. The samples were heated to temperatures from 300 to 1100° (at 100°C intervals) for a time of 10^4 s and then cooled to room temperature for the texture and microhardness measurements and metallography. As previously noted, the range of temperatures examined spans the range from reactor operating temperatures (~300°C) to those temperatures possibly experienced in a postulated accident condition such as LOCA (~1100°C).

Light Optical Metallography

Specimens suitable for light optical metallography were cut from the tubing using a slow-speed diamond saw, mounted using cold mount, and then ground to

Table 1 Chemical analysis of Zr-1 wt%Nb fuel sheathing

Element[a]	*Content*[b]	*Element*	*Content*
Nb	1.025%	Ta	<25
O	1155	Hf	79
Fe	540	Al	25
Cr	110	Si	29
Ni	<35	Zn	<50
Ti	<25	Zr	Bal

[a] B, Cd, Co, Cu, Mg, Mn, Mo, Sn, V, and W contents were <25 ppm.
[b] All results, other than for Nb (weight %), are in parts per million by weight (ppm).

600-grit SiC. The specimens were then swab etched using a solution containing 45 ml HNO_3, 45 ml H_2O and 10 ml HF and examined at 100 and 500× magnifications.

Microhardness Measurements

The microhardness measurements were made using a 50 gf load and a Knoop indentor. A Knoop rather than a Vickers indentor was used in order to obtain information on the anisotropy of microhardness. The Knoop hardness flow surface technique (Wheeler and Ireland, 1966) was used for the determination of the mechanical anisotropy. This technique involves making Knoop hardness impressions on the three orthogonal surfaces of the tube geometry and from these constructing a flow surface based on the Knoop hardness number (KHN). The Knoop hardness number was obtained by measuring the long diagonal of the Knoop impression and then using tables to obtain KHN. Alternatively, the KHN can be calculated from the equation:

$$\mathrm{KHN} = 14{,}229\, L/d^2 \tag{1}$$

where L is the load in grams and d is the length of long diagonal in μm.

Ideally, these hardness tests should be made at temperature after a given heating period. However, producing hardness impressions on the thin wall of fuel sheathing required suitable mounting and metallographic polishing. Therefore, the microhardness tests were performed at ambient temperature after cooling from the heat treatment temperature. The heat treated specimens for microhardness were cut into sections of approximate size 7 × 10 mm. Then, each set of three sections (orientations) were mounted together (in Bakelite) to display all three surfaces (axial, radial and tangential). They were wet polished and etched using similar procedures as for light microscopy. Hardness indentations for six orientations on the three surfaces were made in order to prepare the flow surface diagram. Five or more hardness impressions were made for each section. Figure 1(a) shows the orientation of the Knoop hardness indentations and Figure 1(b) shows an isotropic flow surface (circle with its centre at origin). A full description of the use of this technique for the study of the mechanical anisotropy of zirconium alloy (Zircaloy-4) fuel sheathing can be found in the paper by Northwood and Fong (1983).

Texture Measurements

The crystallographic anisotropy was determined from inverse pole figures (Mueller, Chernock and Beck, 1958). The basis of this method is that intensities from the sample in question are compared with that from a randomly oriented sample.

The X-ray patterns for the texture determination were recorded using a powder diffractometer and graphite monochromated CuK_α radiation. The patterns were recorded over the range 2θ from 30° to 140° using a scan rate of 2° per minute. These diffraction patterns were recorded for both the radial and tangential directions (these directions were parallel to the X-ray beam). Small sections of the fuel sheathing placed side-by-side were used to make the specimen area larger

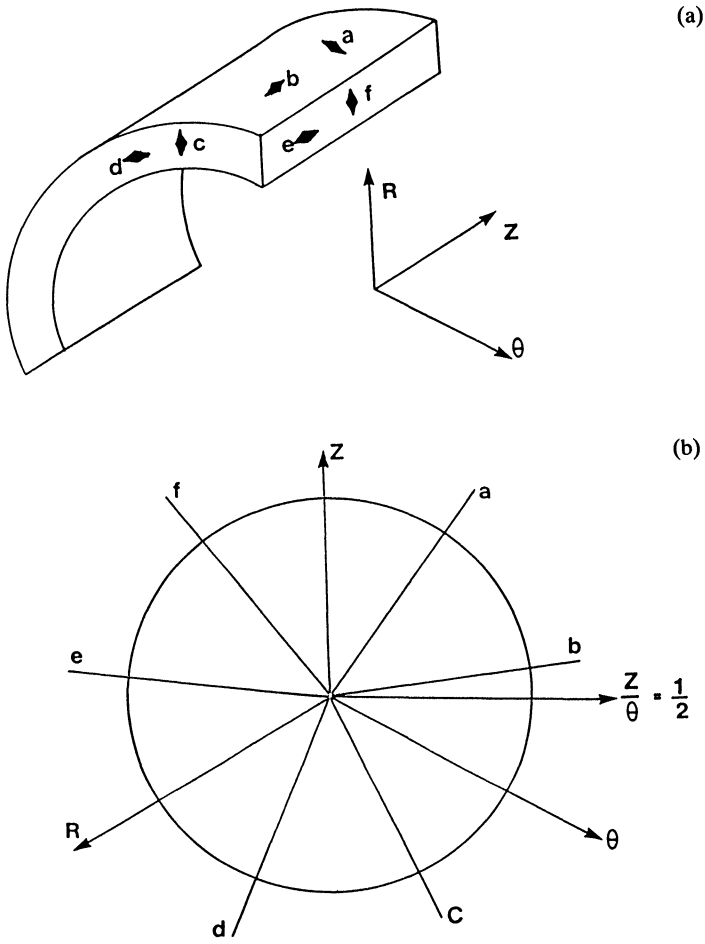

Figure 1 (a) Schematic diagram showing orientations of Knoop hardness indentations in tubing; (b) Isotropic flow surface showing relationship to orientation of Knoop hardness indentations and major directions in tubing.

than the beam area for the radial sample, and four sections glued together were used for the tangential samples. In both cases, the samples were oriented so that the extrusion direction in the tubing was perpendicular to the incident X-ray beam. The randomly oriented sample was a zirconium powder (~325 mesh).

The intensities of all (*hkil*) reflections for the test samples and the randomly oriented zirconium powder sample were determined. A texture coefficient (T.C.) for each (*hkil*) reflection is calculated using the equation (Mueller, Chernock and Beck, 1958):

$$\text{T.C.}_i = \frac{I_i/I_i^0}{1/n \sum^{i=n} I_i/I_i^0} \tag{2}$$

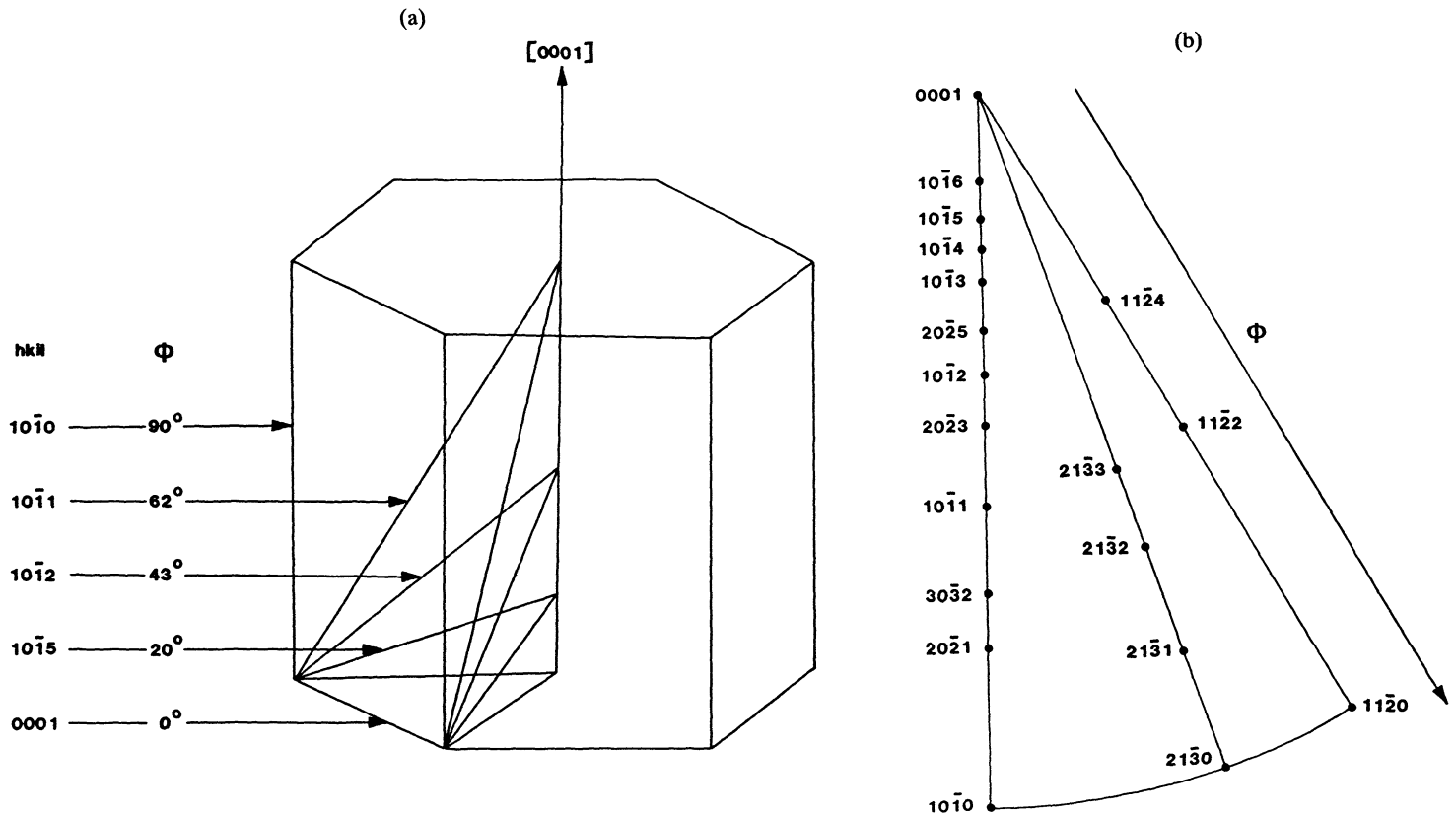

Figure 2 (a) Schematic diagram of the hexagonal prism and the angles between the major (*hkil*) planes and the basal plane; (b) Standard stereographic projection for α-zirconium showing the position of the major *hkil* poles.

where

I_i = experimentally determined intensity of the ith reflection for the textured sample.

I_i^0 = calculated or experimentally determined intensity of the ith reflection from the randomly oriented sample.

These T.C. values are then entered on the standard stereographic projection of α-zirconium (see Figure 2 for schematic diagrams of (a) the hexagonal prism and the angles between major (*hkil*) planes and the basal plane, and (b) a standard stereographic projection for α-zirconium and the position of major *hkil* poles). Other data was extracted from these plots and the type of data and its analysis will be described in more detail in the Experimental Results section.

RESULTS

Light Optical Metallography

In order to better interpret the changes in microstructure occurring on heating for 10^4 s at temperatures from 300°C to 1100°, it is helpful to review the Zr-Nb phase diagram and other details concerning the constitution of Zr-Nb alloys.

The Zr-Nb phase diagram is basically a eutectoid with a solid miscibility gap region (usually described as a monotectoid) and with a minimum liquidus point, Figure 3. It is only the solidus part of the diagram that is of concern to this study because temperatures are limited to 1100°C. The major point of discussion and experiment has been the solid solubility limit of Nb in the hcp α-Zr phase which has been given as low as 0.6 wt%Nb and as high as 6.5 wt%Nb (Northwood and Gillies, 1979).

The oxygen content of Zr-Nb alloys can have a large effect on the position of the phase boundaries. Increasing the oxygen content decreases the solubility of Nb in the α-Zr phase and raises the monotectoid temperature (Kubit, 1970). The main effect of oxygen is to raise the (α-Zr + β-Zr)/β-Zr transformation temperature. For oxygen contents of ~1000 ppm, such as typically found in zirconium alloys produced from sponge zirconium, the maximum solubility of Nb in α-Zr is considered to be ~0.6 wt% and the monotectoid temperature is considered to be ~610°C. Thus, Zr-1 wt%Nb is a two-phase material at room temperature and temperatures up to the transformation to a single phase β-Zr solid solution. The (α-Zr + β-Zr)/β-Zr transus temperature for this batch of Zr-1 wt%Nb alloy has been previously determined as 925 ± 10°C (Northwood, 1974).

Representative micrographs of the fuel sheathing in the as-received condition and after heating for 10^4 s at 500, 600, 700, 900 and 1000°C (followed by air cooling to ambient temperature) are given in Figures 4(a) to (f). Points to be noted from the micrographs are as follows:

- The as-received microstructure, Figure 4(a) consisted of elongated α-Zr grains (light phase) with some β-phase (dark) at the boundaries of the elongated α-grains.
- Recrystallization started at 500°C and was essentially completed at 600°C.

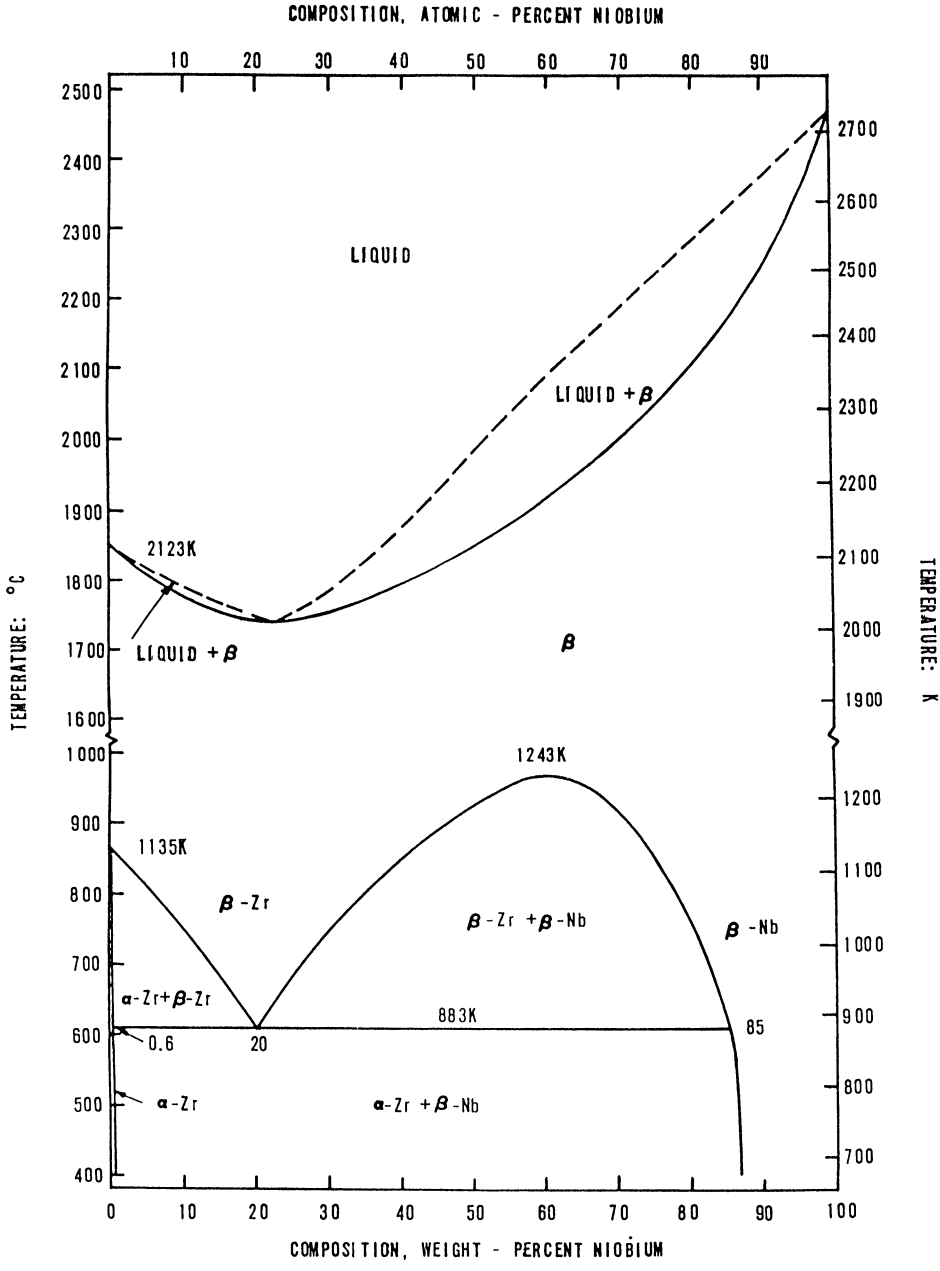

Figure 3 The binary Zr-Nb phase diagram.

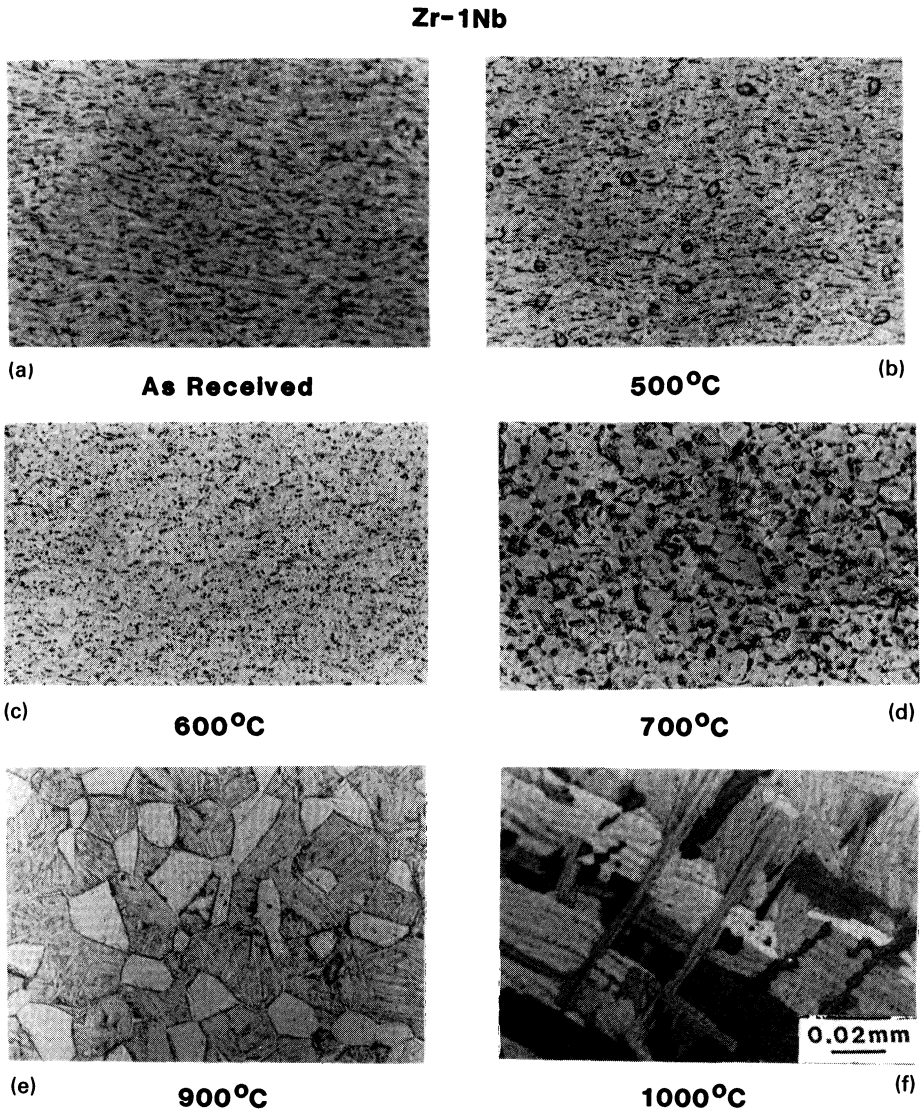

Figure 4 Optical micrographs of structure of cold-worked Zr-1 wt%Nb fuel sheathing after heating for 10^4 s at the indicated temperatures followed by air cooling to ambient temperature.

The distribution of the β-phase was changed little compared to the as-received material.

• Heating the alloy at 700 to 900°C brought it above the monotectoid temperature into the $\alpha + \beta$-Zr phase region. The volume fraction of β-Zr was higher after treatment at 900°C than after treatment at 700°C. The β-Zr was unstable and transformed, at least partially, to an α structure on cooling to room temperature. This is shown in Figures 4(d) and 4(e) where the

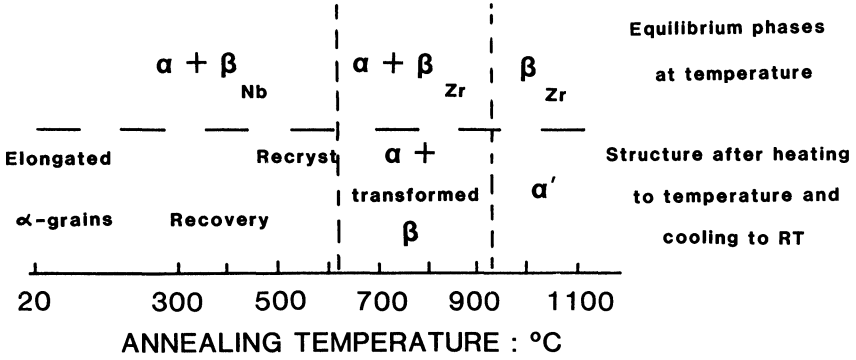

Figure 5 Schematic representation of the effect of annealing temperature on the equilibrium phases present at temperature and the structure produced by heating for 10^4 s followed by cooling to ambient temperature.

transformed β-phase (dark) was the minor constituent after 700°C treatment but the major constituent after 900°C treatment.

- Heating at 1000°C brought the alloy into the single-phase β-Zr region. Cooling to room temperature produced an α' structure (basketweave or parallel-plate Widmanstatten structure, Figure 4(f).

The phases present at temperature, and the structures produced by cooling to ambient temperature after 10^4 s at temperature, are summarized in Figure 5.

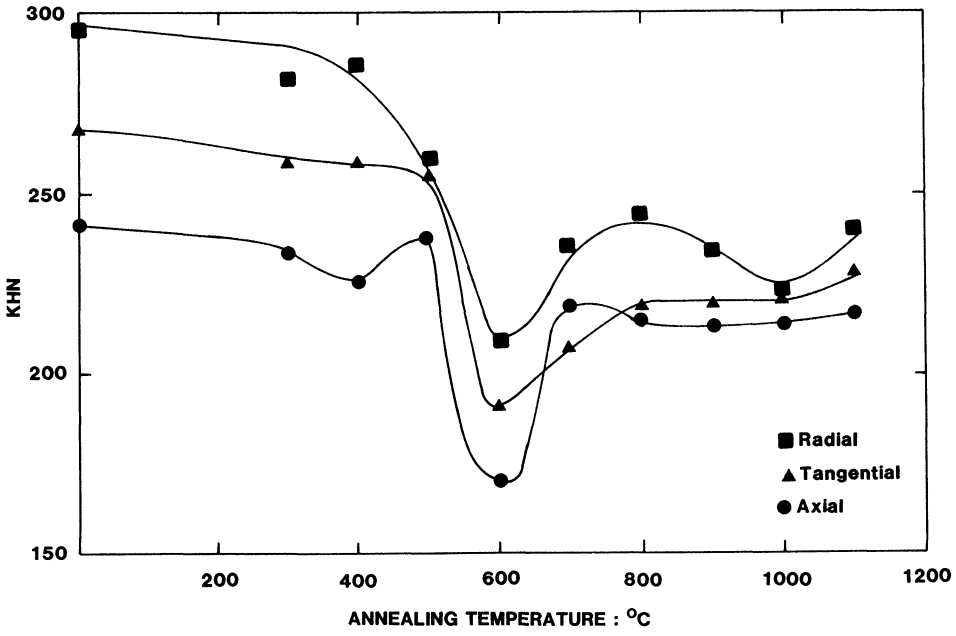

Figure 6 Dependence of the microhardness in the three principal directions on the annealing temperature.

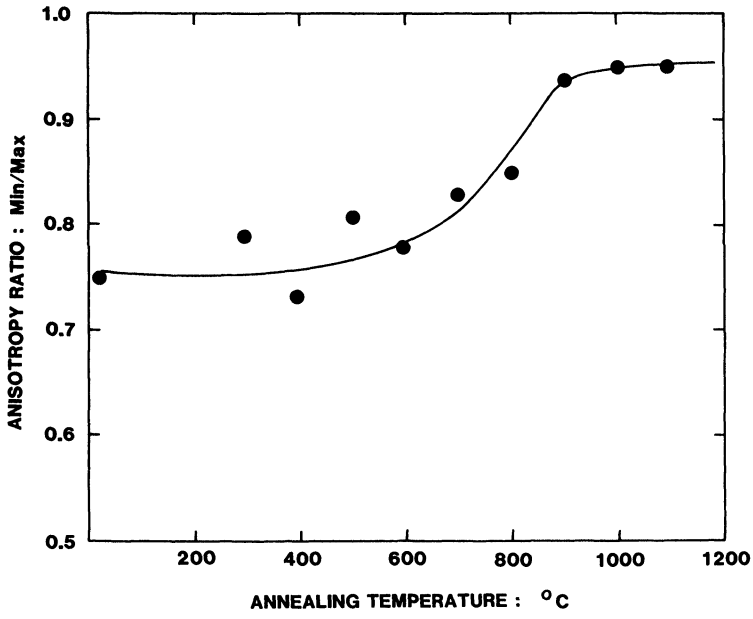

Figure 7 Dependence of the mechanical anisotropy ratio on the annealing temperature.

Microhardness Measurements

Values of microhardness (in KHN) for all three directions in the tubing are given in Figure 6 as a plot of KHN vs. annealing temperature. The same general trends are noted for all directions. There is a large decrease in microhardness for annealing temperatures of 400 to 600°C. The microhardness then increases again from 600 to 800°C, remains reasonably constant from 800 to 1000°C before increasing again at 1100°C. The microhardness variations are also illustrated as a plot of anisotropy ratio (ratio of minimum to maximum microhardness) vs. annealing temperature, Figure 7. The anisotropy ratio is relatively unchanged for temperatures up to ~600°C, increases significantly between 600°C and 900°C and then remains approximately constant for 900–1100°C (i.e., there is a general trend towards more isotropic mechanical properties as the annealing temperature increases).

Texture Measurements

The inverse pole figures for all annealing conditions are given in Figure 8 for the radial direction and in Figure 9 for the tangential direction. These figures show the T.C. values for each pole; the identification of *hkil* for each T.C. value can be found in Figure 2(b). There appears to be little, if any, changes in these inverse pole figures, and hence in the texture, for annealing temperatures of 500°C and below: this is true for both the radial and tangential data. There are texture changes for annealing temperatures $\lesssim$600°C and at 900°C–1000°C the material

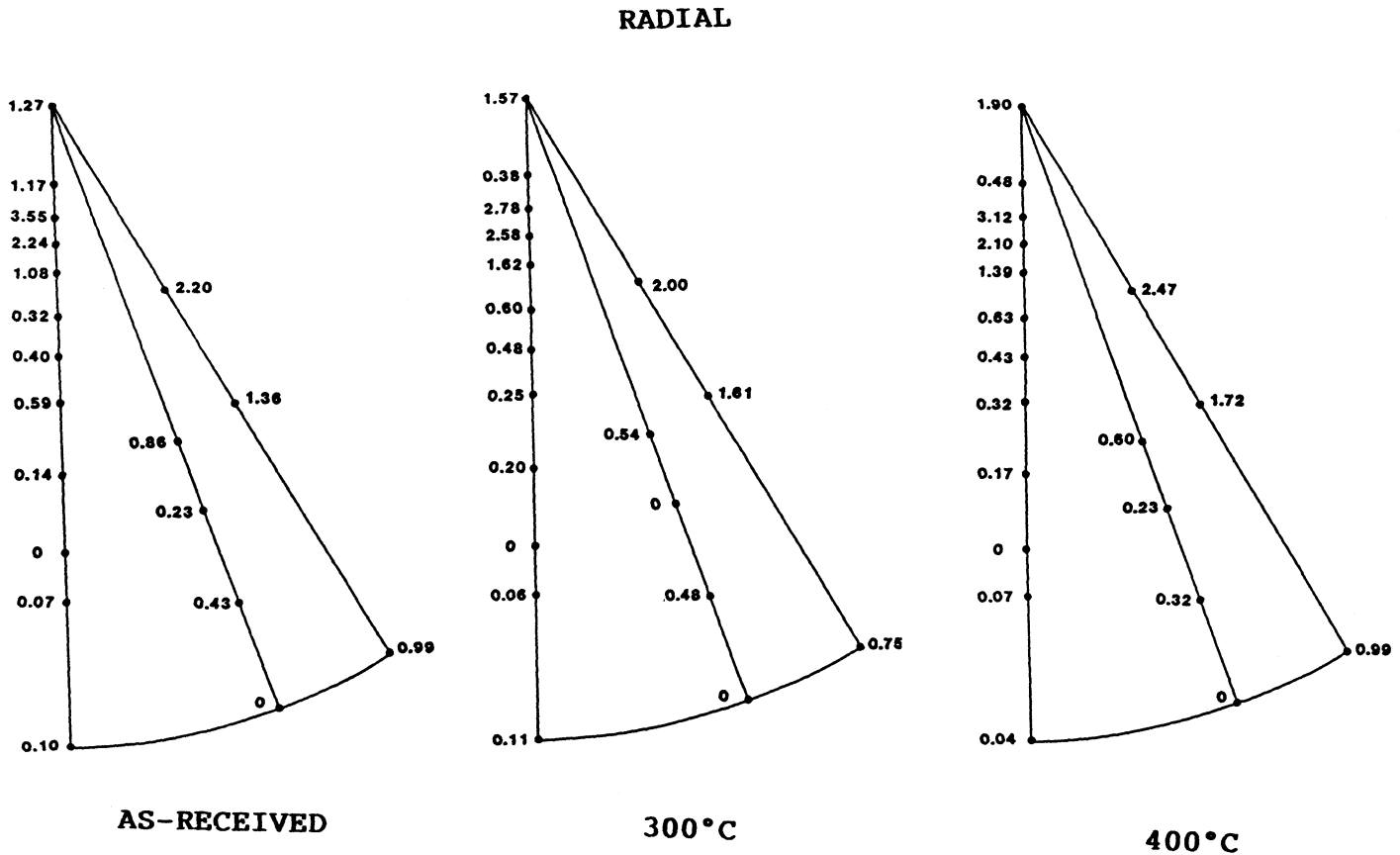

Figure 8 Inverse pole figures for the radial direction for cold-worked Zr-1 wt%Nb fuel sheathing after heating for 10^4 s at indicated temperature and cooling to ambient temperature.

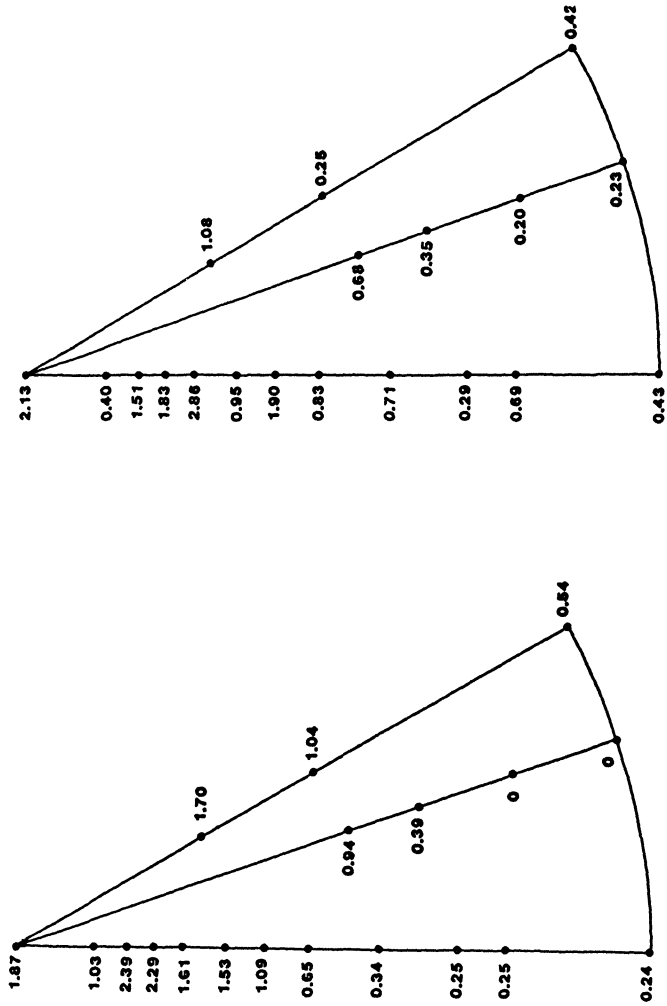

Figure 8 (*Continued*)

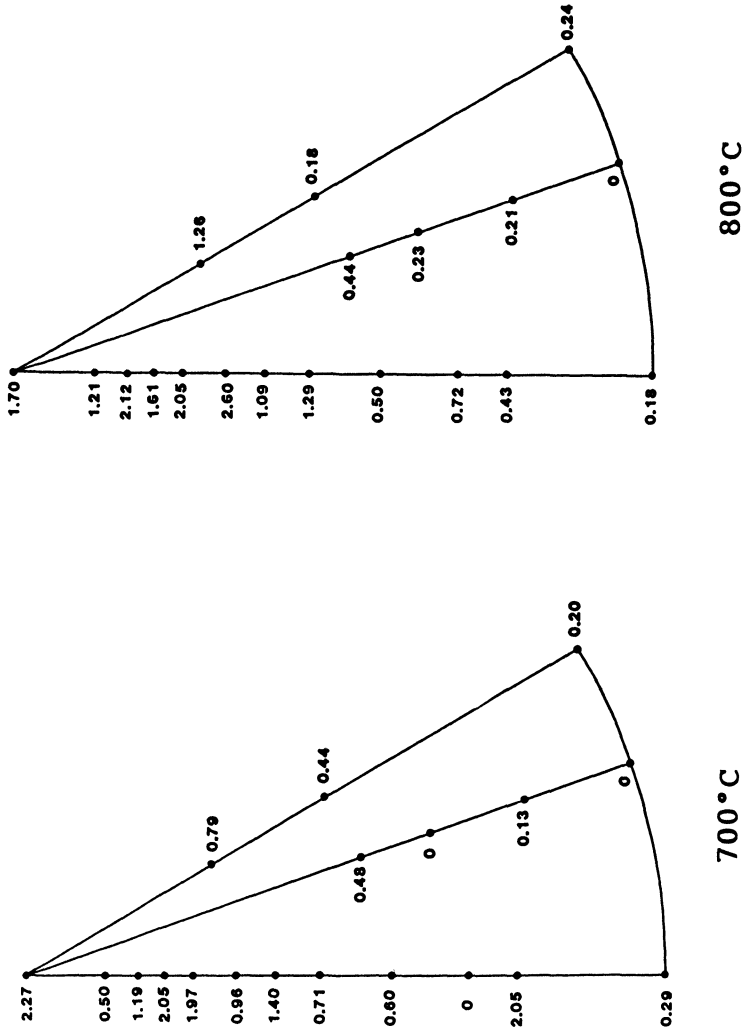

Figure 8 (*Continued*)

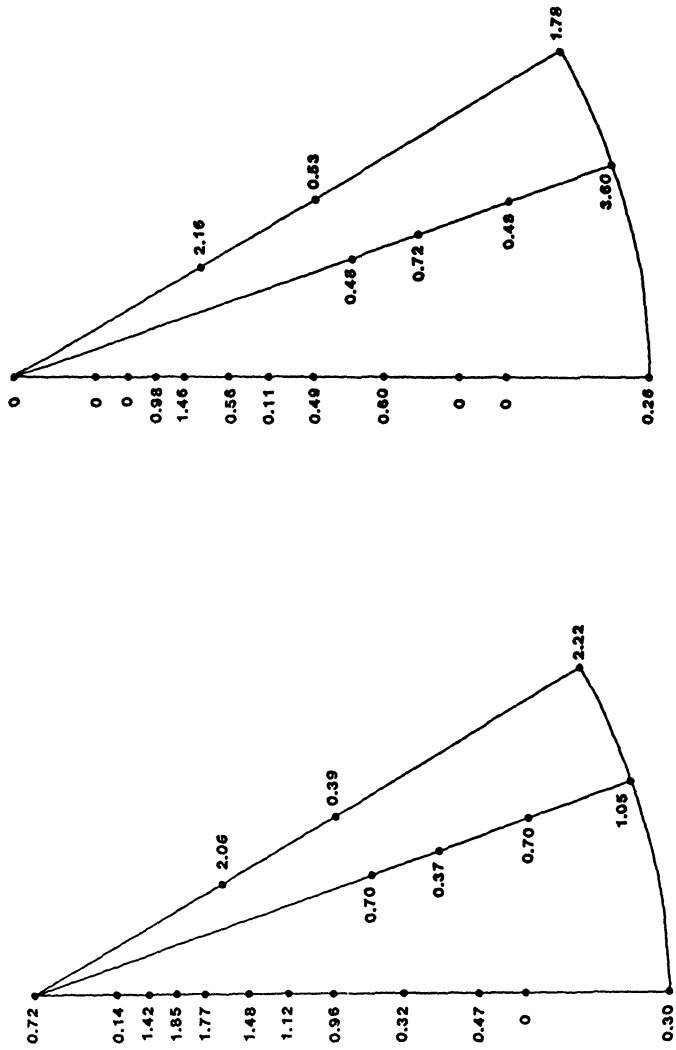

Figure 8 (*Continued*)

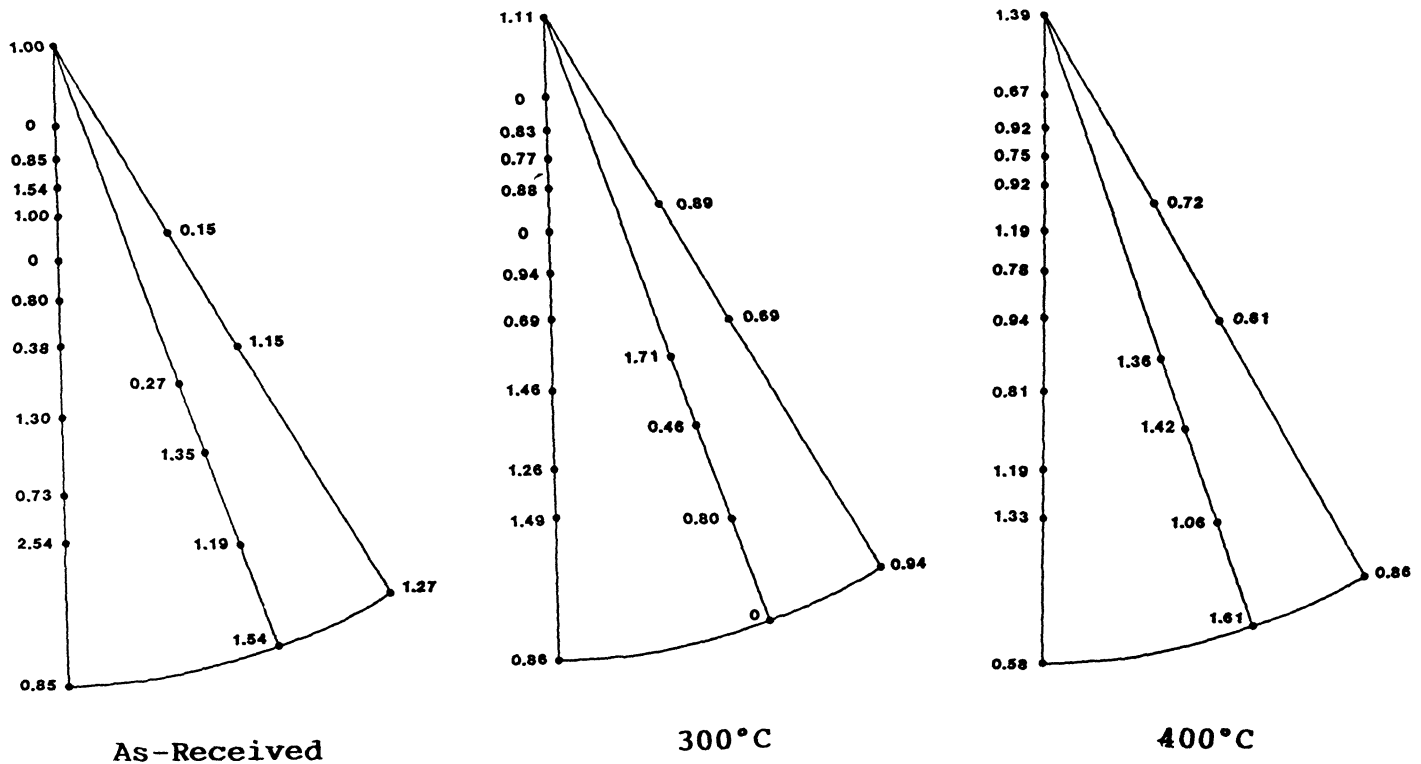

Figure 9 *Inverse pole figures for the tangential direction for cold-worked Zr-1 wt%Nb fuel sheathing after heating for* 10^4 *s at indicated temperature and cooling to ambient temperature.*

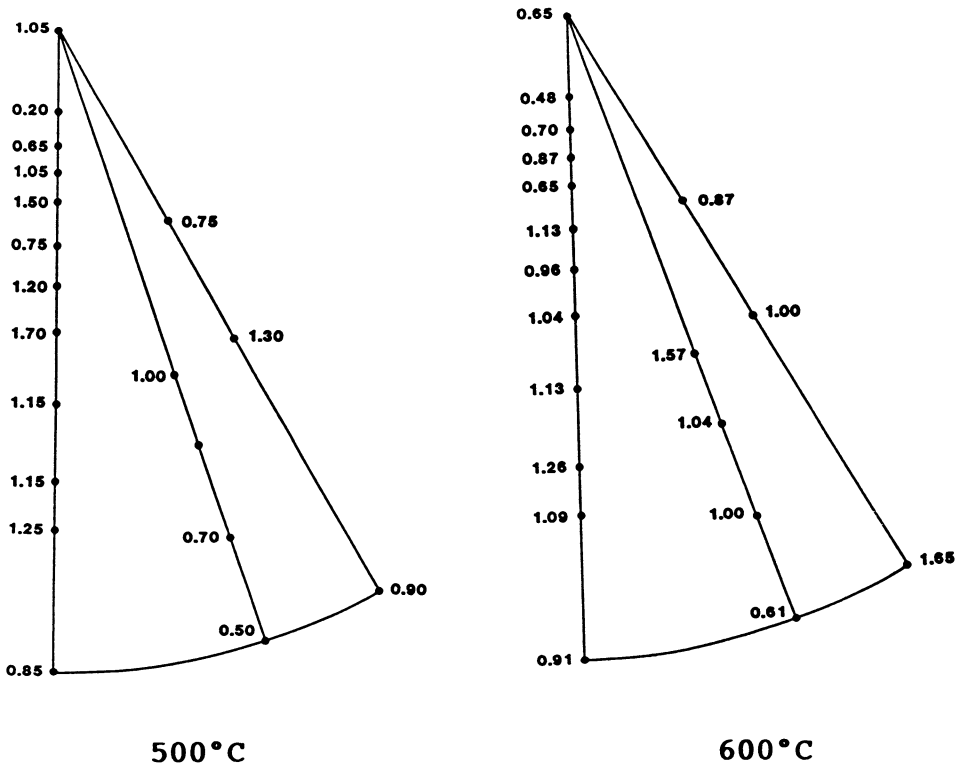

Figure 9 (*Continued*)

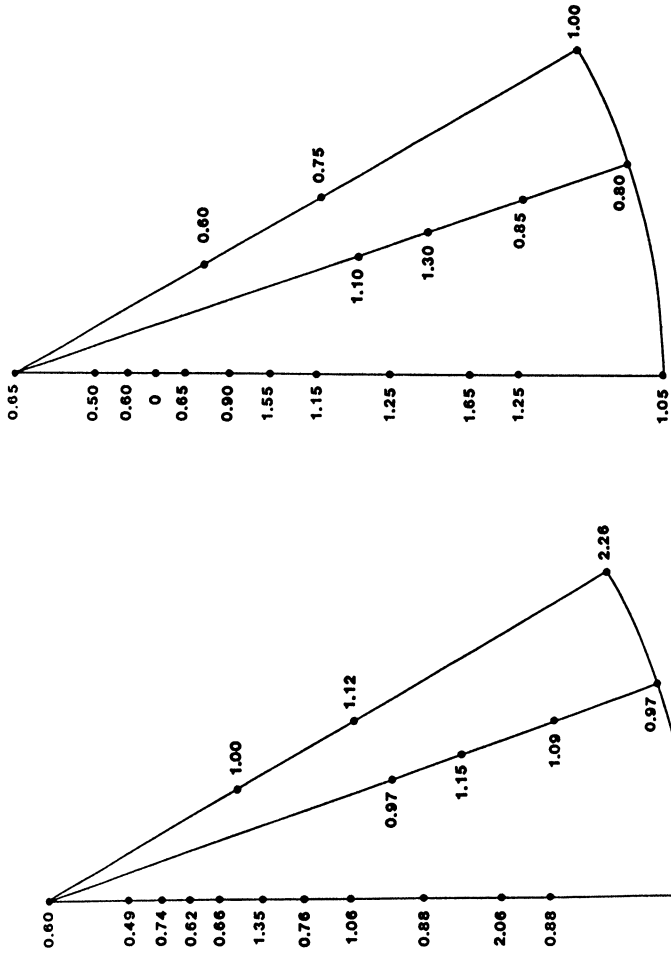

Figure 9 *(Continued)*

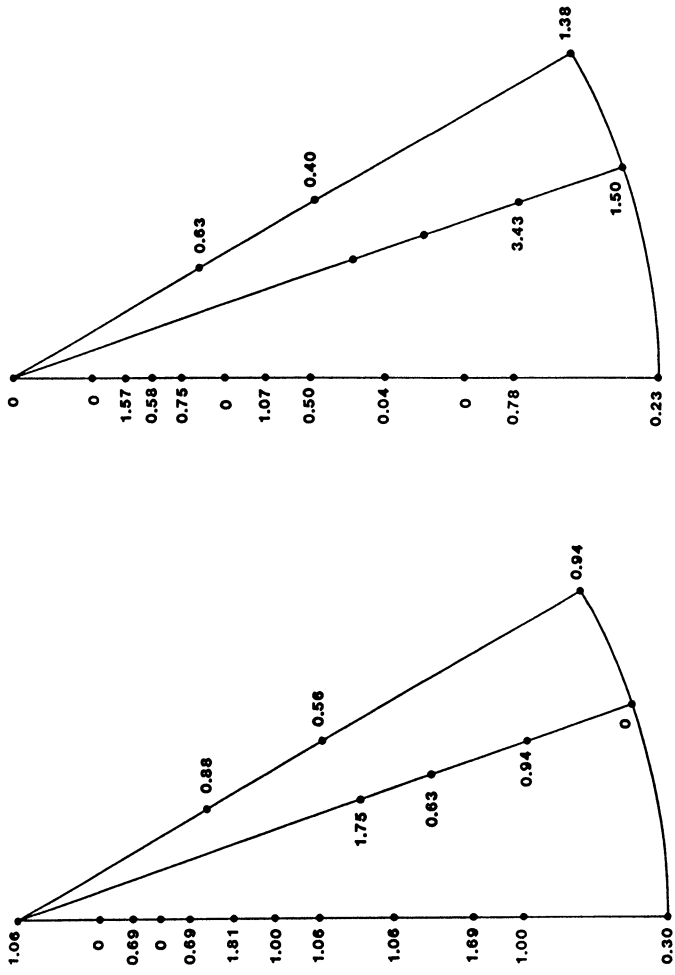

Figure 9 (*Continued*)

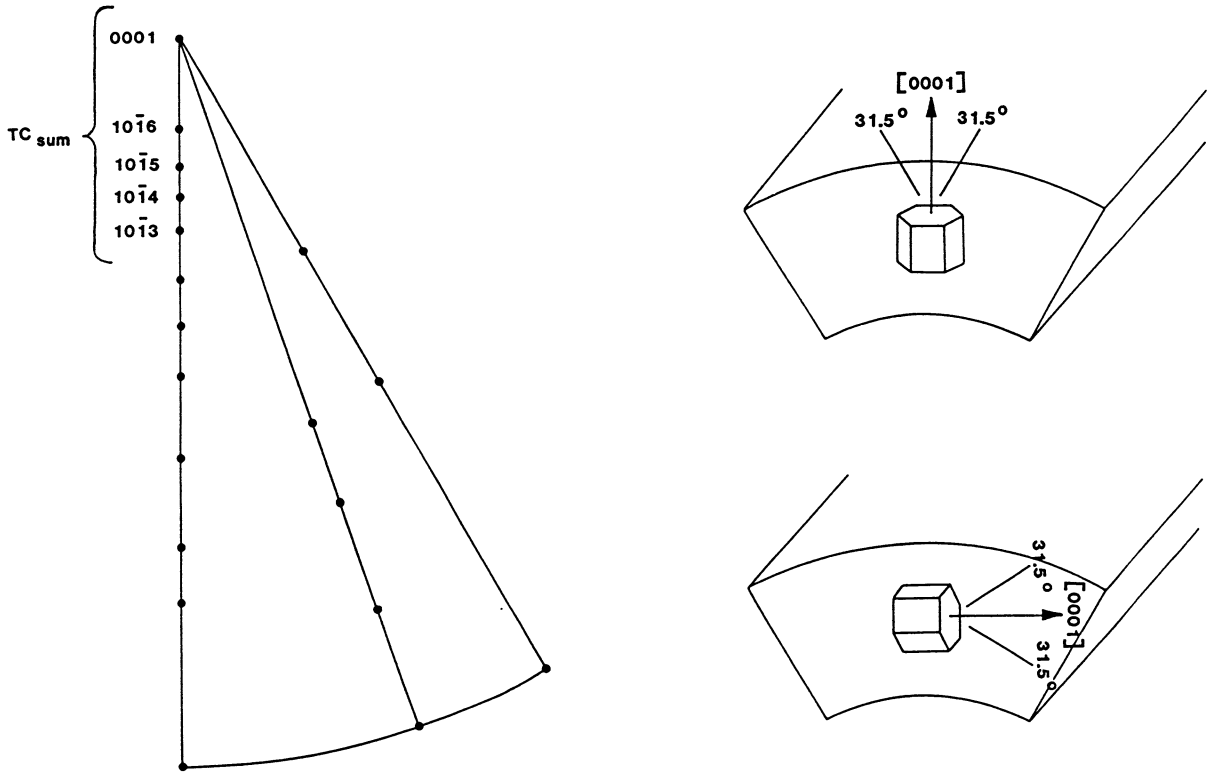

Figure 10 Schematic diagram showing the location of the poles used for the TC_{sum} both within the fuel sheathing and on the inverse pole figure.

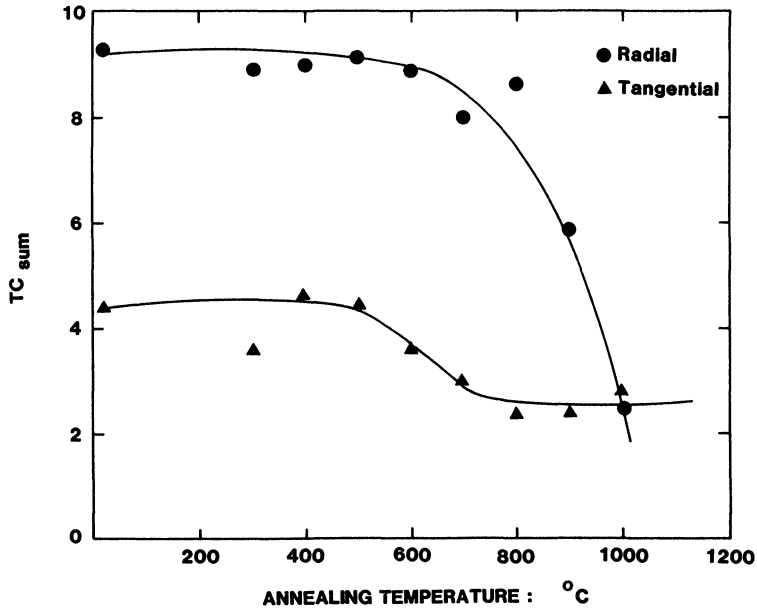

Figure 11 Dependence of the TC_{sum} (Texture Coefficient Sum) for the radial and tangential directions in fuel sheathing on the annealing temperature.

becomes less textured as evidenced by most of the T.C. values being neither very much greater nor much smaller than 1.

In order to 'highlight' some of the changes occurring in the texture, use is made of a parameter called TC_{sum}. The TC_{sum} is the sum of the texture coefficients for the planes, the poles of which are oriented in [0001] or within ±31.5° of this direction: see Figure 10 for schematic diagram showing the orientation of these poles within the fuel sheathing and the location of these poles on the inverse pole figure. Looking at the values for TC_{sum} for the radial and tangential directions, Figure 11, it can be seen that there is little change in TC_{sum} until the annealing temperature exceeds 600°C when both TC_{sum} (radial and tangential) decrease. The TC_{sum} for radial and tangential directions are approximately equal for an annealing temperature of 1000°C.

RELATIONSHIPS BETWEEN MECHANICAL ANISOTROPY, TEXTURE AND MICROSTRUCTURE

The changes experienced by the Zr-1 wt%Nb fuel sheathing on annealing at temperatures up to 1100°C can be divided into two main categories, namely those associated with the removal of cold-work (i.e., recovery and recrystallization) and those associated with any phase changes. In general, the removal of cold-work occurs at the lower temperatures, i.e., ≲600°C, and, for the heating period (10^4 sec) used in this study, no significant phase changes occur until the monotectoid temperature, ~610°C (Northwood & Gillies, 1979) is exceeded.

The recovery process which occurs at annealing temperatures of 300°C and 400°C produced very little, if any, effect on the properties measured in the study. There was a small decrease in the microhardness values (compared to the as-fabricated tubing) but the mechanical anisotropy ratio and the texture (as seen in the TC_{sum} values for the radial and tangential directions) remained essentially unchanged. Recovery effects were, of course, not visible using optical metallography. One of the better techniques for monitoring these recovery effects has proven to be thermoelectric power measurements and results for the Zr-1 wt%Nb can be found in the paper by Jie, Robinson and Northwood (1989).

Recrystallization, which occurs at 500°C and 600°C, produces a number of changes which were monitored in this study. Recrystallization is readily seen in the optical micrographs, see Figure 4. It also produces a very significant drop in the microhardness levels for all three principal directions in the tubing, see Figure 6. However, there was no significant change in the mechanical anisotropy ratio, Figure 7. The changes in texture, as reflected in TC_{sum} values, were also small during recrystallization: there is a drop in TC_{sum} for the tangential direction between 500°C and 600°C.

Major changes in the anisotropy, both mechanical and crystallographic, were not found until the annealing temperature exceeded 600°C. It is in this temperature range that one crosses a phase boundary (the monotectoid temperature) between the α-Zr + β-Nb and the α-Zr + β-Zr phase regions (Northwood and Gillies, 1979). Once this boundary has been crossed, the amount of β-Zr (actually transformed β in the samples cooled back to ambient temperature) also increases.

As the volume fraction of transformed β-phase increases there is an increase in the microhardness, Figure 6. Also as the amount of transformed β-phase increases, the tubing becomes more mechanically isotropic reaching a mechanical anisotropy ratio of 0.95 (1.0 is isotropic) for a structure consisting of 100% transformed beta, Figure 7. This trend is also seen in the crystallographic anisotropy (texture) in that the TC_{sum} for the radial direction, which has the highest number of grains with their basal poles (and poles oriented up to 31.5° from this direction) oriented in this direction, drops sharply for annealing temperatures greater than about 600°C, Figure 11. This isotropy is further shown by the fact that the TC_{sum} values are essentially the same for the radial and tangential directions for the specimen annealed at 1000°C which has a 100% transformed-β structure).

CONCLUSIONS

The changes occurring in cold-worked Zr-1 wt%Nb fuel sheathing during annealing for 10^4 sec at temperatures from 300°C to 1100°C and cooling to ambient temperature have been monitored using Knoop microhardness, optical metallography and X-ray texture measurements. For annealing temperatures up to ~600°C, i.e., below the transformation temperature for α-Zr + β-Nb $\rightarrow$ α-Zr + β-Zr, there is little change in texture or mechanical anisotropy ratio. The tubing merely becomes softer due to recrystallization and the removal of cold-work. As the annealing temperature is increased and the amount of β

(actually transformed-β) increases, the tubing becomes harder and more mechanically isotropic reaching an anisotropy ratio of 0.95 (1.0 is isotropic) for a structure consisting of 100% transformed-β. This trend in mechanical anisotropy is also reflected in the texture in that the TC_{sum} for the radial direction, which has the highest number of grains with their basal poles (and poles oriented up to 31.5° from this direction) oriented in this direction, drops sharply for annealing temperatures greater than about 600°C. For a structure consisting of 100% transformed-β, TC_{sum} values for the radial and tangential directions are essentially the same.

Acknowledgements

The Zr-1 wt%Nb fuel sheathing was kindly supplied by Atomic Energy of Canada Limited. Funding for this study was provided by the Natural Sciences and Engineering Research Council of Canada through Operating Grant No. A4391.

References

Amaev, A. D. *et al.* (1964). Influence of some factors upon hydriding and variation of properties of zirconium alloy with 1%Nb used for fuel element cladding in water-moderated water-cooled power reactors. In *Proc. 3rd Int. Conf. on Peaceful Uses of Atomic Energy*, p. 342. Geneva: IAEA.

Amaev, A. D. *et al.* (1966). Investigation of an assembly of rod type fuel elements with sintered UO_2 with zirconium alloy cladding with maximum burnup of 68,000 MWd/Tu. In *Proc. Conf. on the Use of Zirconium Alloys in Nuclear Reactors*, Paper 7. Marianske Lazne, Czechoslovakia. (also published as Kurchatov Inst. Report IAE-1181 (1966) and Atomic Energy Commission Translation AEC-TR-6847).

Amaev, A. D. *et al.* (1968). Investigation of the behaviour of zirconium alloys in water and steam-water mixture in the MR reactor loops. In *Proc. Zirconium '68 Meeting*, Paper 3. Marianske Lazne, Czechoslovakia.

Jie, Z., Robinson, J. R. and Northwood, D. O. (1989). A metallographic study of annealing of Zr-1 wt%Nb nuclear fuel sheathing. *Microstructural Science*, **17**, 393–404.

Kubit, C. J. (1970). A study of phase transformations in zirconium-rich Zr-Nb alloys containing oxygen. Ph.D. Thesis, University of Pittsburgh.

Mueller, M. H., Chernock, W. P. and Beck, P. A. (1958). Comments on inverse pole figure methods. *Trans. Metallurgical Society AIME*, **212**, 39–40.

Northwood, D. O. (1974). Zr-1 wt%Nb as a fuel sheathing in water-cooled reactors. Chalk River Nuclear Laboratories Report CRNL 947. Chalk River, Ontario, Canada: AECL.

Northwood, D. O. (1985). The development and applications of zirconium alloys. *Materials and Design*, **VI** (2), 58–70.

Northwood, D. O. and Fong, W. L. (1983). Effect of brazing on mechanical anisotropy of Zircaloy-4 nuclear fuel cladding. *Canadian Metallurgical Quarterly*, **22**, 411–419.

Northwood, D. O. and Gillies, D. C. (1979). A determination of the $\alpha/(\alpha+\beta)$ and $(\alpha+\beta)/\beta$ phase boundaries in the zirconium-niobium system. *Microstructural Science*, **7**, 123–132.

Wheeler, R. G. and Ireland, D. R. (1966). Multiaxial plastic flow of Zircaloy-2 determined from hardness data. *Electrochemical Technology*, **4**, 313–317.